Environmental controls of frost cracking revealed through in situ acoustic emission measurements in steep bedrock

Girard, Lucas; Gruber, Stephan; Weber, Samuel; Beutel, Jan

DOI: https://doi.org/10.1002/grl.50384

GEOPHYSICAL RESEARCH LETTERS, VOL. 40, 1748–1753, doi:10.1002/grl.50384, 2013

Environmental controls of frost cracking revealed through in situ acoustic emission measurements in steep bedrock

Lucas Girard,[1] Stephan Gruber,[1] Samuel Weber,[2] and Jan Beutel[2]

Received 18 December 2012; revised 12 March 2013; accepted 17 March 2013; published 15 May 2013.

[1] Frost cracking, the breakdown of rock by freezing, is one of the most important mechanical weathering processes acting on Earth's surface. Insights on the mechanisms driving frost cracking stem mainly from laboratory and theoretical studies. Transferring insights from such studies to natural conditions, involving jointed bedrock and heterogeneous thermal and hydrological properties, is a major challenge. We address this problem with simultaneous in situ measurements of acoustic emissions, used as proxy of rock damage, and rock temperature/moisture content. The 1 year data set acquired in an Alpine rock wall shows that (1) liquid water content has an important impact on freezing-induced rock damage, (2) sustained freezing can yield much stronger damage than repeated freeze-thaw cycling, and (3) that frost cracking occurs over the full range of temperatures measured extending from 0 down to –15°C. These new measurements yield a slightly different picture than previous field studies where ice segregation appears to play an important role. **Citation:** Girard, L., S. Gruber, S. Weber, and J. Beutel (2013), Environmental controls of frost cracking revealed through in situ acoustic emission measurements in steep bedrock, *Geophys. Res. Lett.*, *40*, 1748–1753, doi:10.1002/grl.50384.

1. Introduction

[2] The progressive damage and fracture of rock exposed to freezing is a fundamental problem with broad implications in geosciences. It plays a crucial role in periglacial landscape evolution by sediment production through physical weathering and has affected large parts of the Earth under colder climate [*Matsuoka and Murton*, 2008; *Anderson*, 1998]. Frost cracking is also hypothesized to play an important role in the destabilization of steep permafrost [*Gruber and Haeberli*, 2007], representing a major hazard potential in populated mountainous areas. This is also critical in engineering since frost damage affects the durability of concrete structures [*Basheer et al.*, 2001].

[3] As frost cracking operates slowly in the field, it has mostly been approached by laboratory experiments [e.g., *Hallet et al.*, 1991; *Murton et al.*, 2006] and theoretical studies [*Walder and Hallet*, 1985; *Vlahou and Worster*, 2010; *Røyne et al.*, 2011]. These studies have demonstrated that frost weathering can result from the operation of two different mechanisms, (1) the 9% volumetric expansion of freezing water and (2) ice segregation, a mechanism also responsible for frost heave in soils, yielding slow growth of ice inside rock under sustained freezing conditions. This is caused by disjoining forces, repelling the infilled-ice from the surrounding rock [*Dash et al.*, 1995]. These forces lower the pressure in unfrozen water films adjacent to the ice surface inducing water migration toward the solidification front. Over time, this fuels the growth of segregated ice in cracks and induces stresses that can eventually cause ice-filled cracks to widen. Volumetric expansion requires a significant saturation level to generate stresses [*Prick*, 1997]. It occurs at temperatures close to 0°C although this can be locally affected by freezing point depression and can be partially relieved by ice creep and extrusion over time [*Krautblatter et al.*, 2013]. Contrastingly, ice segregation can occur at temperatures considerably below 0°C that were estimated to range from –4 to –15 °C based on numerical simulations considering low porosity rocks [*Walder and Hallet*, 1985]. Although it does not require a specific water saturation level to take place, segregated ice growth is constrained by the availability of liquid water.

[4] Insights from such fundamental studies on frost cracking have been used as a basis to investigate the phenomenon at a larger geomorphic scale [*Anderson*, 1998; *Hales and Roering*, 2007]. These studies seek to understand potential locations of segregated ice growth by estimating the time that rock spends within a temperature interval (–8 to –3°C). A proxy of frost cracking intensity is then estimated from the cumulative time spent in this so-called frost cracking window [*Anderson*, 1998], or as a product of the temperature gradient with the time spent in the cracking window [*Hales and Roering*, 2007]. There is however little field evidence to guide such a transfer of the laboratory and theoretical insights on frost cracking to natural conditions with heterogeneous thermal, hydrological, and mechanical properties. This points out the need for direct field observations of frost cracking, along with simultaneous monitoring of relevant environmental parameters.

[5] Here we address this problem using measurements of in situ rock damage, temperature, and liquid water content from a high-alpine rock wall. We characterize the impact of different thermal regimes (freeze-thaw cycling, sustained freezing) and liquid water contents on rock damage. We show that frost cracking is unlikely to be restricted to the frost cracking window and that water availability has a critical impact on the resulting damage.

Additional supporting information may be found in the online version of this article.

[1]Glaciology and Geomorphodynamics, Department of Geography, University of Zurich, Switzerland.

[2]Computer Engineering and Networks Laboratory, Swiss Federal Institute of Technology Zurich, Switzerland.

Corresponding author: L. Girard, Glaciology and Geomorphodynamics, Department of Geography, University of Zurich, Switzerland. (lucas.girard@geo.uzh.ch)

0094-8276/13/10.1002/grl.50384

2. Methods

[6] Acoustic emissions (AEs) are transient elastic waves that are generated by the rapid release of energy within a material, through crack formation or friction between solid surfaces [*Hardy*, 2003]. In a previous pilot study, we have demonstrated the feasibility of using AE monitoring to capture freezing-induced rock fracture under natural conditions [*Amitrano et al.*, 2012]. This pilot study showed that AE generated by freezing-induced stresses can indeed be detected and that the statistical properties of AE correspond to those of microfracturing.

[7] The characteristics of the acoustic signals generated by rock failure processes are controlled by the scales of rupture dimension and displacement. These two scales can be seen as the typical size of rock joints and the size of displacement at the crack tip during a rupture event, respectively. Here, we focus on rupture dimensions on the order of 1–10 cm and rupture displacements of 0.1–1 μm. These scales determine the frequency range of the AE signals to be detected, yielding here 20–100 kHz. In this range of frequencies, AE signals are attenuated over distances of 0.5–1 m in rock.

[8] In order to monitor AE signals in this frequency range, from specific depths of a rock wall, over a year long period, we have used a custom-built system that consists of (1) the AE-node, a two-channel acquisition system with wireless data transmission [*Girard et al.*, 2012], and (2) special casings that house AE sensors inside boreholes and allow to retrieve acoustic signals from specific depths [*Weber et al.*, 2012]. We have chosen to install the AE sensors at depths of 10 and 50 cm. This choice was motivated by the fact that frost weathering can be expected to be more active in the near-surface than at greater depths. Second, the detection ranges of the two sensors overlap, so that a simple zonation of AE source depth can be performed.

[9] The AE Node operates as a standard AE acquisition system: it continuously samples the signal $V(t)$ with a frequency of 500 kHz. The signal analysis is triggered by the crossing of a threshold, defining the beginning of an event, which ends when the threshold has not been exceeded for 400 μs. Each AE event is parametrized following the standard terminology [*Hardy*, 2003]; here we restrict our analysis to two of these parameters: the maximal signal amplitude A_i of each event i, and the energy E_i, defined as the integral of $V^2(t)$ for the duration of the event.

[10] The measurement system is completed by two additional probes that measure rock temperature at six levels (5, 10, 20, 30, 50, and 100 cm) and rock moisture content, through capacitive measurements at three levels (10, 20, and 50 cm). Details on the measurements system are provided in the auxiliary material and in *Girard et al.* [2012].

3. Measurement Site

[11] The measurement site is a south-facing rock wall located near Jungfraujoch, in the central Swiss Alps, at an elevation of 3500 m above sea level. The site is next to the high-altitude research station Jungfraujoch and can be accessed year-round by train. The 50–70° steep wall is composed of densely fractured crystalline rock [*Wegmann and Keusen*, 1998]. The mean annual rock temperatures near the surface are between –2 and –3°C in this south face. Throughout the year, the near-surface of this rock wall encounters strongly contrasting thermal conditions with a period of sustained freezing in winter (lasting typically 2 months), freeze-thaw cycling in spring and autumn, and fully thawed conditions in summer [*Hasler et al.*, 2011]. The densely fractured rock shows about 5–20 joints per meter, with apertures from 0.5 mm to 1 cm. AEs in the range of frequency detectable by the AE Node are expected to be generated mainly by these joints. Moreover, the large joint density ensures that several joints are within the detection range of each AE sensor. An interjoint porosity of 1–2% was measured from drill core plugs.

[12] Two measurement systems, each composed of a two-channel AE Node, temperature and moisture probes, were deployed on the rock wall. The deployment locations are about 10 m apart and show similar general characteristics (Figure 1 and the auxiliary material). The main difference between these two locations lies in the expected rock liquid water availability. The first measurement system, referred to as M1, is on a rather dry spur-like feature protruding from the main wall by a meter. The second one (M2) is in a gully-like depression (about a meter deep) that is prone to collect meltwater from snow patches above. The distance between both locations (10 m) is an order of magnitude larger than the detection range of AE sensors (0.5 m). Therefore, the AE activity detected at one location is independent from that of the second location. The waveform and frequency content of one of the AE events detected by the system are shown as example in Figure 1.

4. Freezing-induced Change of Rock Physical Properties

[13] The velocity and the attenuation of elastic waves in rock is known to vary upon freezing due to changing properties of the joint and pore infill [*Timur*, 1968]. Additionally, the pressure exerted by the growth of ice in rock pores and cracks upon freezing was shown to have a considerable impact on seismic velocities [*Draebing and Krautblatter*, 2012]. Similarly, the distance over which elastic waves are attenuated in frozen rock can be expected to be larger than under thawed conditions. Such changes in rock properties may increase the probability of detecting AE events under frozen conditions. In order to quantify this effect, transmission tests were carried out using rock core plugs taken at both measurement locations. Based on these results, an empirical correction was applied to the detected AE parameters, as detailed in the auxiliary material.

5. Elementary Classification of AE Events

[14] As we cannot ensure that all AE events detected at the field site are real acoustic emissions generated by rock damage processes, we first review possible sources of spurious events before providing further data analysis. While the AE sensors are housed inside the rock wall and are to some extent protected from external noise, snow avalanches as well as toppling of small debris could have contributed to generate spurious AE events. These effects would however be limited to specific time periods since (1) the slope accumulates very little snow and avalanche activity mostly occurs in the late spring, and (2) toppling rocks are most expected in summer when larger areas of the slope are snow free. In order to perform an elementary classification of

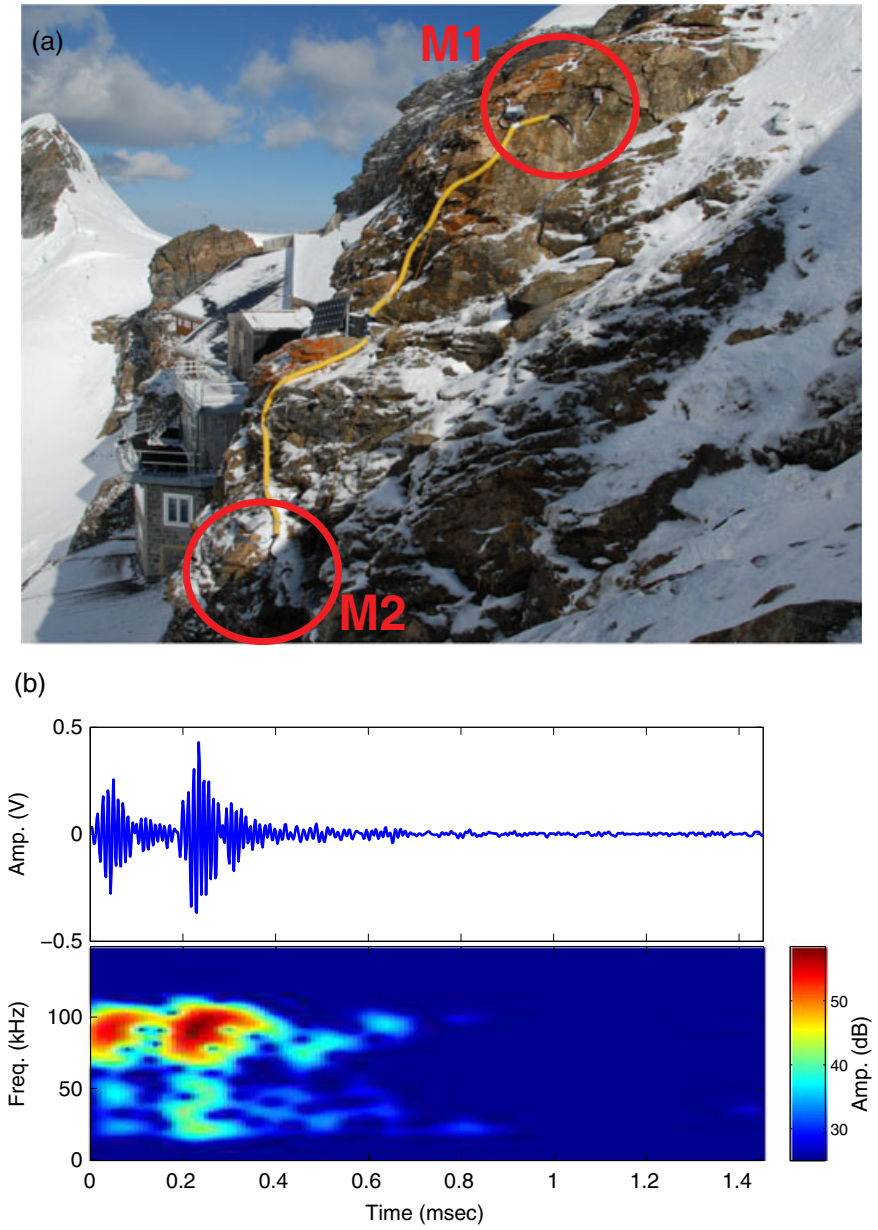

Figure 1. (a) Field site overview at Jungfraujoch showing both measurement locations, M1 and M2. (b) Example of signal waveform and frequency content of an AE event detected by the system.

AE events that are most likely associated with rock damage processes, we use an analogy with the properties of AE events detected during laboratory rock fracturing experiments. Following *Cox and Meredith* [1993], we reject all events having a duration/amplitude ratio less than one-tenth of the average value. This allows to reject events with very large amplitudes but very small durations, which are typically caused by noise.

[15] Ice filling the rock joints and cracks could also contribute to generate spurious AE events, under creep/plastic deformation [*Weiss and Louchet*, 2006] or melting [*Sakharov*, 1994]. However, such events would be several orders of magnitude smaller in energy than AE generated from centimeter-scale flaws in rock. Ice growth in rock cavities will tend to induce tensile stresses at crack tips of the embedding rock, and in reaction, infilled ice will encounter compressive stress states. The brittle failure of ice and rock is well captured by the Coulomb failure criterion [*Weiss and Schulson*, 2009], with larger compressive than tensile strength. Additionally, the tip of the rock crack will act as a stress concentrator. Therefore, it is reasonable to assume that rupture is more likely to occur in rock than in the infilled ice [*Amitrano et al.*, 2012]. Finally, we recall that infilled ice can only reach a maximal volumetric fraction of 1–2% of this low porosity rock.

6. Results

[16] The two measurement systems have been operating since Fall 2011; here we report data acquired during a 1 year period extending from October 2011 to September 2012. Throughout that period, a total of about 6.5×10^5 events were detected by both AE Nodes, out of which 2.2×10^5 fulfill the duration/amplitude ratio classification criterion. We

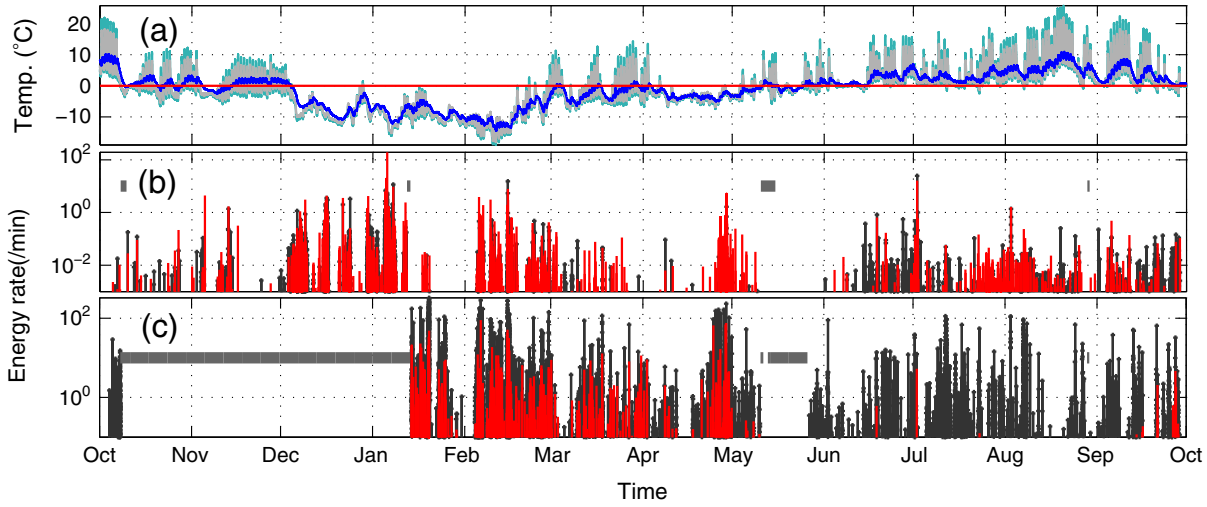

Figure 2. Time series of (a) rock temperatures measured at 5 (green), 10 (grey), and 50 cm (blue) depth at M2. Rates of AE energy detected at (b) M1 and (c) M2 at 10 cm (black) and 50 cm (red). Horizontal gray bars denote periods where the monitoring system did not operate correctly due to technical problems.

report the AE activity as a rate of AE energy, computed as the total energy of AE events detected during a minute, at a given depth and location (Figure 2). AE activity occurred in discontinuous bursts at both measurement locations throughout the year. However, the mean AE energy rates detected under positive rock temperatures ($T > 0$ over the entire depth range, from 5 to 100 cm) are no more than a few percent of the energy rates detected below the datum freezing point ($T < 0$ over the entire depth range) (Table 1). A burst-shaped pattern of AE activity was reported in the pilot study, and a correlation analysis showed that it was the expression of temporal event clustering [*Amitrano et al.*, 2012], a property that is commonly observed for fracturing heterogeneous materials.

[17] We now compare two neighboring periods of 32 days with contrasting freezing conditions: P1 from 28th January to 29th February; subzero temperatures were measured at all depths during the whole period at both locations. On the other hand, during P2 from 29th February to 1st March, 17 freeze-thaw cycles were detected at 10 cm depth at M1, and 18 cycles at M2 (Figure 2). At both locations and both depths, the total AE energy detected during P1 (sustained freezing) was about 10 times larger than for P2 (freeze-thaw cycling). Note that this discrepancy cannot be directly related to the cumulative time of freezing, since during the second period, the total time of subfreezing temperatures at 10 cm depth is about 23 days (72% of the whole period). Additionally, we note that the total time spent in the previously postulated frost cracking window ($-8 < T < -3$°C) was shorter for P1 (6.7 days) than for P2 (11.1 days), with respect to temperature at 10 cm depth at M1 (comparable numbers were obtained at 50 cm and at M2).

[18] We examine differences between the two measurement locations: under freezing conditions, the mean energy rates observed at M2 are always larger than at M1 (by a factor of 5 at 50 cm depth, for example). In order to relate these differences to possible discrepancies in rock liquid water content, we analyze measurements obtained from the capacitance probes (Figure 3). As detailed in *Girard et al.* [2012], the probes could not be calibrated to absolute values in this low porosity rock. Despite of that, uncalibrated readings of the probe are still useful to compare relative liquid water contents of the two locations. These measurements confirm higher liquid water content at M2 (gully) than at M1 (spur). As the measurements are sensitive to liquid water content, this difference could translate in discrepancies in saturation levels and/or in the local porosity. Although we could not quantify the porosity accurately (including that of joints), the morphology of the drill cores suggests a higher joint density at M2 than at M1 (see the auxiliary material).

[19] One may note that mean energy rates detected under freezing at 50 cm depth at M1 are larger than at 10 cm, expressing a stronger AE activity at depth than closer to the surface. On the other hand, the opposite case is observed at M2. This could be related to local differences in the liquid water content, since larger water contents can be expected to promote frost cracking [*Matsuoka and Murton*, 2008]. However, this could not be elucidated based on the measurements of the capacitance probes, which are not sensitive enough to resolve such small and local differences. Local topographic settings may partly explain these results: the spur-like feature of M1 receives almost no surface meltwater and very seldom retains snow, contrary to the gully of M2, which tends to collect meltwater and may accumulate snow

Table 1. Mean Rates of AE Energy (/Day) Detected on Each Channel of Both Monitoring Systems, for All Temperature Conditions (All), for AE Activity Detected During Periods Where All Temperature Measurements (5–100 cm Depth) are Negative (Frozen), and AE Activity Detected for Periods Where All Temperature Measurements are Positive (Thawed)[a]

	All	Frozen	Thawed
M1, 10 cm	0.28	1.07	0.015
M1, 50 cm	0.84	3.10	0.013
M2, 10 cm	1.65×10^2	3.30×10^2	15.53
M2, 50 cm	7.21	16.07	0.0083

[a]Events detected simultaneously on both channels of a given measurement location have been excluded, so that energy rates reported here are independent from each other.

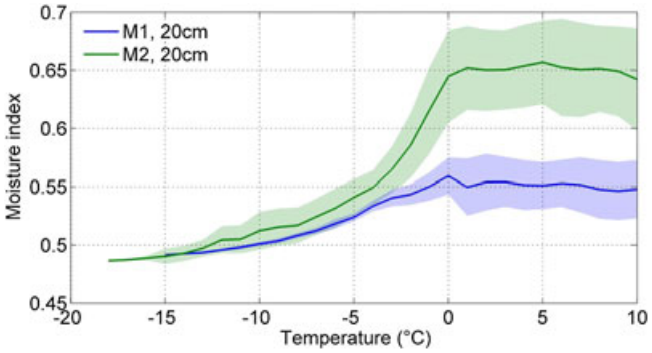

Figure 3. Moisture index defined as the average normalized reading of the capacitance probe at 20 cm depth, for bins of the rock temperature measured at the same depth near the probe. Colored surface areas correspond to standard deviations. Measurements obtained between October 2011 and September 2012 were considered. Probe readings were corrected for their temperature dependence as detailed in *Girard et al.* [2012].

(Figure 1). The water input could therefore occur mainly by percolation through the rock mass at M1, which may explain the larger AE activity at depth there, while opposite conditions occur at M2 where the surface is directly exposed to water and larger AE activity occurs close to the surface.

[20] We finally analyze variations in detected AE energy rates for bins of the temperature (Figure 4). This analysis is based on AE events detected at 50 cm depth only; events detected on both sensors have been excluded. This is motivated by the fact that at larger depth, temperature gradients are smaller. Therefore, by selecting only the deeper events, we can be more confident that the temperature close to the sensor is representative of the temperature at the source that generated the AE event. Large energy rates were detected on the whole range of subzero temperatures encountered, extending down to –15°C. At both locations, there is an abrupt decrease in energy rates above 0°C, followed by increasing values at higher positive temperatures.

7. Discussion and Conclusions

[21] The results presented show that both freezing and fully thawed conditions can generate AE activity. In the later case, the AE activity may be partly affected by stress inherited from previously frozen rock. Thermomechanical forcing (rock thermal expansion/contraction), arising from heterogeneities in the temperature field, is also a likely driver of rock damage under thawed conditions. Thermomechanical forcing is known to contribute to fracture propagation on a wide range of depths [*Gischig et al.*, 2011]. In our field study, such thermomechanical effects cannot be disentangled from freezing-induced mechanisms. However, we have shown that rates of AE energy detected under freezing conditions are about two orders of magnitude larger than under thawed conditions. This suggests that AE activity detected during subzero periods can be attributed to a large extent to freezing-induced processes, so that it can be interpreted as the expression of frost cracking. In addition, the statistical properties of AE events correspond to that of microfracturing, as detailed in the pilot study [*Amitrano et al.*, 2012].

[22] Although we cannot strictly quantify the range of rock saturation levels encountered during the monitoring period, our results suggest that even under relatively dry near-surface conditions (M2 location), the operation of frost weathering could be detected through AE activity. In this case, freezing-induced damage is likely associated with water migration within the frozen rock, since in situ water content would not be high enough to induce damage upon freezing [*Prick*, 1997]. A second important aspect of the results reported is the illustration that sustained freezing can yield much stronger frost cracking activity than repeated freeze-thaw cycling. This aspect also argues for the importance of water migration fueling the growth of ice during such periods of sustained freezing. Finally, the fact that large

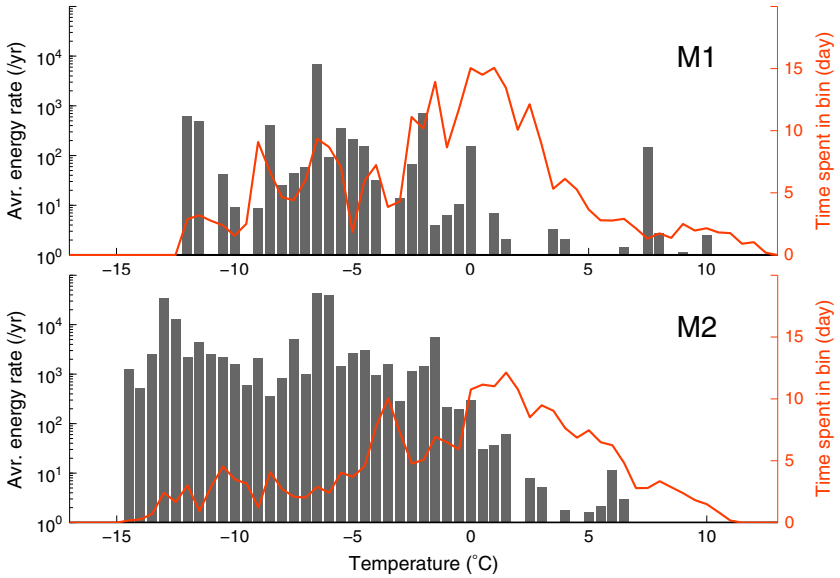

Figure 4. Average rates of AE energy detected at 50 cm depth for bins of the temperature (grey bars) for both locations. Rates were obtained by normalizing the total detected AE energy by the total time spent in each temperature bin (red curve).

rates of AE energy were detected at temperatures considerably below 0°C also suggests that water migration and ice segregation play an important role [*Walder and Hallet*, 1985].

[23] However, AE activity was also shown to take place just below freezing and during short freezing periods, which could be the expression of in situ freezing. Previous field studies, based on measurements of crack widening at the rock surface, emphasized the importance of in situ volumetric expansion, especially due to refreezing of snowmelt water infiltrating the crack during seasonal thawing [*Matsuoka*, 2008]. Such measurements were obtained from the surface only, and from single cracks. Here AE measurements allowing to track the evolution of damage within the rock mass yield a slightly different picture where ice segregation appears to play a more important role. Finally, we report that the time spent in the frost cracking window [*Anderson*, 1998] does not appear to be a relevant proxy of freezing-induced rock damage. More measurements will be required to investigate if considering the temperature gradient within the frost cracking window, as suggested by *Hales and Roering* [2007] can improve this or if a different modeling framework should be used to evaluate the large-scale geomorphic implications of frost cracking.

[24] **Acknowledgments.** The research presented was supported through the project CracklingMap funded by the Forschungskredit of the University of Zurich and the project PermaSense funded by the Swiss National Foundation (SNF) NCCR MICS. Support from the International Foundation High Altitude Research Stations Jungfraujoch and Gornergrat is also acknowledged. The authors are grateful to David Amitrano for constructive discussions.

References

Amitrano, D., S. Gruber, and L. Girard (2012), Evidence of frost-cracking inferred from acoustic emissions in a high-alpine rock-wall, *Earth Planet. Sci. Lett.*, *341-344*, 86–93, doi:10.1016/j.epsl.2012.06.014.

Anderson, R. S. (1998), Near-surface thermal profiles in alpine bedrock: Implications for the frost-weathering of rock, *Arctic Alpine Res.*, *30*, 362–372.

Basheer, L., J. Kropp, and D. J. Cleland (2001), Assessment of the durability of concrete from its permeation properties: A review, *Construct. Build. Mater.*, *15*, 93–103, doi:10.1016/S0950-0618(00)00058-1.

Cox, S. J. D., and P. G. Meredith (1993), Microcrack formation and material softening in rock measured by monitoring acoustic emissions, *Int. J. Rock Mech. Min. Sci.*, *30*(1), 11–24.

Dash, J., H.-Y. Fu, and J. Wettlaufer (1995), The premelting of ice and its environmental consequences, *Rep. Progr. Phys.*, *58*, 115–167.

Draebing, D., and M. Krautblatter (2012), *P*-wave velocity changes in freezing hard low-porosity rocks: A laboratory-based time-average model, *The Cryosphere*, *6*, 1163–1174, doi:10.5194/tc-6-1163-2012.

Girard, L., J. Beutel, S. Gruber, J. Hunziker, R. Lim, and S. Weber (2012), A custom acoustic emission monitoring system for harsh environments: Application to freezing-induced damage in alpine rock walls, *Geosci. Instrum. Method. Data Syst.*, *1*, 155–167, doi:10.5194/gi-1-155-2012.

Gischig, V. S., J. R. Moore, K. F. Evans, F. Amann, and S. Loew (2011), Thermomechanical forcing of deep rock slope deformation: 1. Conceptual study of a simplified slope, *J. Geophys. Res.*, *116*, F04010, doi:10.1029/2011JF002006.

Gruber, S., and W. Haeberli (2007), Permafrost in steep bedrock slopes and its temperature-related destabilization following climate change, *J. Geophys. Res. Earth Surf.*, *112*(F02S18), 10, doi:10.1029/2006JF000547.

Hales, T. C., and J. J. Roering (2007), Climatic controls on frost cracking and implications for the evolution of bedrock landscapes, *J. Geophys. Res.*, *112*, F02033, doi:10.1029/2006JF000616.

Hallet, B., J. S. Walder, and C. W. Stubbs (1991), Weathering by segregation ice growth in microcracks at sustained sub-zero temperatures: Verification from an experimental study using acoustic emissions, *Permafrost Periglac.*, *2*(4), 283–300.

Hardy, H. (2003), *Acoustic Emission/Microseismic Activity - Principles, Techniques and Geotechnical Applications*, A. A. Balkema, Lisse, Netherlands.

Hasler, A., S. Gruber, and W. Haeberli (2011), Temperature variability and thermal offset in steep alpine rock and ice faces, *The Cryosphere*, *5*, 977–988, doi:10.5194/tc-5-977-2011.

Krautblatter, M., D. Funk, and F. K. Gunzel (2013), Why permafrost rocks become unstable: A rock-ice-mechanical model in time and space, *Earth Surf. Proc. Land.,* doi:10.1002/esp.3374.

Matsuoka, N. (2008), Frost weathering and rockwall erosion in the southeastern Swiss Alps: Long-term (1994–2006) observations, *Geomorphology*, *99*, 353–368.

Matsuoka, N., and J. B. Murton (2008), Frost weathering: Recent advances and future directions, *Permafrost Periglac.*, *19*, 195–210.

Murton, J. B., R. Peterson, and J. C. Ozouf (2006), Bedrock fracture by ice segregation in cold regions, *Science*, *314*(5802), 1127–1129.

Prick, A. (1997), Critical degree of saturation as a threshold moisture level in frost weathering of limestones, *Permafrost Periglac.*, *8*, 91–99.

Røyne, A., P. Meakin, A. Malthe-Sørenssen, B. Jamtveit, and D. K. Dysthe (2011), Crack propagation driven by crystal growth, *EPL*, *96*(24003), doi:10.1209/0295-5075/96/24003.

Sakharov, I. I. (1994), Nature of acoustic emission during phase transformations and adequacy of the Stefan condition, *J. Eng. Phys. Thermophys.*, *67*, 699–702.

Timur, A. (1968), Velocity of compressional waves in porous media at permafrost temperatures, *Geophysics*, *33*, 584–595, doi:10.1190/1.1439954.

Vlahou, I., and M. G. Worster (2010), Ice growth in a spherical cavity of a porous medium, *J. Glaciol.*, *56*(196), 271–277.

Walder, J., and B. Hallet (1985), A theoretical model of the fracture of rock during freezing, *Bull. Geol. Soc. Am.*, *96*, 336–346.

Weber, S., S. Gruber, L. Girard, and J. Beutel (2012), Design of a measurement assembly to study in-situ rock damage driven by freezing, *Proceeding of the 10th International Conference on Permafrost,* Salekhard, Russia, pp. 437–442.

Wegmann, M., and H. R. Keusen (1998), Recent geophysical investigations at a high alpine permafrost construction site in Switzerland, *Proceedings of the Seventh International Conference on Permafrost, Yellowknife, Northwest Territories, Canada*, pp. 1119–1123.

Weiss, J., and F. Louchet (2006), Seismology of plastic deformation, *Scripta Mater.*, *54*, 747–751.

Weiss, J., and E. M. Schulson (2009), Coulombic faulting from the grain scale to the geophysical scale: Lessons from ice, *J. Phys. D Appl. Phys.*, *42*(214017), doi:10.1088/0022-3727/42/21/214017.